THE JOURNAL OF PHYSICAL CHEMISTRY C

pubs.acs.org/JPCC

Article

Controlling Surfactant Adsorption on Highly Charged Nanoparticles to Stabilize Bijels

Stephen Boakye-Ansah, Mohd Azeem Khan, and Martin F. Haase*

Cite This: J. Phys. Chem. C 2020, 124, 12417−12423

Read Online

ACCESS | Metrics & More | Article Recommendations | Supporting Information

ABSTRACT: Bicontinuous particle-stabilized emulsions (bijels) are networks of interpenetrating oil/water channels with applications in catalysis, tissue engineering, and energy storage. Bijels can be generated by arresting solvent transfer induced phase separation (STrIPS) via interfacial jamming of nanoparticles. However, until now, STrIPS bijels have only been formed with silica nanoparticles of low surface charge densities, limiting their potential applications in catalysis and fluid transport. Here, we show how strongly charged silica nanoparticles can stabilize bijels. To this end, we carry out a systematic study employing dynamic light scattering, zeta potential, acid/base titrations, turbidimetry, surface tension, and confocal microscopy. We find that moderating the adsorption of oppositely charged surfactants on the particles is crucial to facilitate particle dispersibility in the bijel casting mixture and bijel stabilization. Our results potentially introduce a general understanding for bijel fabrication with different inorganic nanoparticle materials of variable charge density.

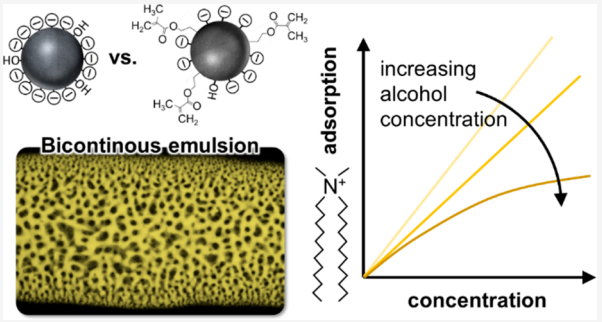

INTRODUCTION

Bicontinuous interfacially jammed emulsion gels (bijels) have found numerous uses as batteries,[1−3] filters,[4] tissue engineering scaffolds,[5] ultralight materials,[6,7] and catalytic microreactors.[8,9] Bijels consist of two continuous liquid phases arranged within an intertwined channel network. This out-of-equilibrium structure is stabilized by a rigid film of colloidal particles at the liquid−liquid interface.[10,11] Bijels can be generated either via spinodal phase separation[10,12,13] or vigorous agitation of two immiscible fluids.[14,15] In both cases, colloidal particles stabilize the liquid network via interfacial jamming due to the enormous particle attachment energies equaling thousands of kT.[16]

Bijel stabilization is not trivial, since the colloidal particles are required to have equal wettability by both liquid phases, expressed by a three-phase contact angle close to 90°.[17,18] This requires precise control over the particle surface chemistry. Traditionally, equal wettability has been achieved via controlled colloid drying protocols[10] or covalent colloid surface hydrophobization.[19,20] Recently, the surface chemistry of colloids has been adjusted by the physisorption of oppositely charged surfactants,[12,14,15] also known as *in situ* modification.[21] This approach is straightforward and versatile, since no time-consuming pretreatments of the particles are needed. Moreover, a broad range of different particle types can be employed to stabilize bijels via *in situ* modification. For instance, cationic quaternary ammonium salt surfactants adsorb electrostatically on silanol groups of silica particles, rendering their surface partially hydrophobic and suitable for bijel stabilization.

Nevertheless, until now, only silica particles of low surface charge densities (<1 $\mu C/cm^2$) have been successfully *in situ* modified to stabilize bijels.[4,8,12,22,23] However, it is highly desirable to generate bijels with particles of significantly higher surface charge densities, as this can facilitate applications of bijels in catalysis[8] and electrokinetic fluid transport.[24] The challenge in forming bijels with strongly charged particles lies in the incompatibility of the particles with the bijel casting liquid and the limited control over surfactant adsorption on the particles.

Here, we show how combining *in situ* surface modification with organosilane silica particle pretreatment allows for generating bijels with strongly charged silica particles. In part 1 of this work, we analyze the *in situ* surface modification of silica particles with different charge densities by didecyldimethylammonium bromide (di-C_{10}TAB) in water. We show that the adsorption of di-C_{10}TAB can be moderated by partially functionalizing the strongly charged silica particles with 3-trimethoxypropyl methacrylate (TPMA).[22] In part 2, we show that the TPMA modification allows for dispersibility of the charged silica particles in the bijel casting mixture composed of isopropanol (IPA), water, and diethyl phthalate (DEP). We

Received: February 19, 2020
Revised: May 9, 2020
Published: May 12, 2020

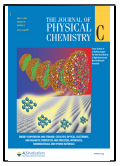

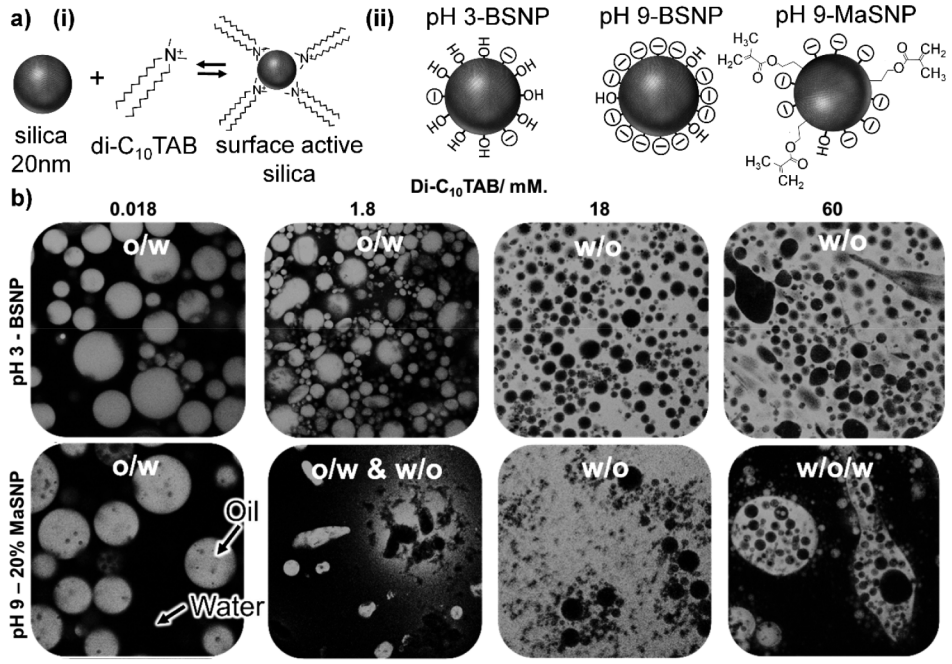

Figure 1. Emulsification behavior of *in situ* modified silica particles. (a) Schematics of (i) the silica particle interaction with di-C_{10}TAB and (ii) different types of silica particles investigated here. (b) Confocal micrographs of shear emulsified oil/water mixtures made of 1:1 (v:v) water (black) and diethyl phthalate (fluorescent gray) with 1 wt % particles at different di-C_{10}TAB concentrations in water.

demonstrate that colloidal stability in this complex fluid mixture results from a combined effect of the solvent and the TPMA modification on the *in situ* surfactant adsorption. Last, we demonstrate the use of solvent transfer induced phase separation (STrIPS) to generate bijel fibers with strongly charged silica particles.

EXPERIMENTAL SECTION

Materials. Ludox TMA (34 wt %), Ludox TM-50 (50 wt %), didecyldimethylammonium bromide (Di-C_{10}TAB), diethyl phthalate (DEP, 99.5%), isopropanol (IPA, >99.7%), toluene (99.8%), Nile red (technical grade), and trimethoxy propyl methacrylate (TPMA, 98%) were purchased from Sigma-Aldrich and used as received.

Methods. Three different types of silica particles, (i) Ludox TMA particles at pH 3 (pH3-BSNP), (ii) Ludox TM-50 particles at pH 9 (pH9-BSNP), and (iii) TPMA modified silica at pH 9 (pH9-MaSNP) are used accordingly. Different combinations of the cationic surfactant, di-C_{10}TAB, and each of the silica particles with different surface properties were used accordingly to prepare ternary mixtures and colloidal suspensions.

Preparation of Silica Nanoparticles. Methacrylate functionalized silica nanoparticles (MaSNPs) are prepared using a protocol from the literature.[22] Calculated amounts of 3-trimethoxypropyl methacrylate (TPMA) are added to a nitrogen purged mixture comprising ethanol (38.1 v/v), water (33.3 v/v), acetic acid (33.3 v/v), and Ludox TMA (9.5 v/v). After 12 h at 70 °C, water is added to the mixture to induce particle agglomeration. The sediment is washed with pure water via centrifugation (9000 rcf, 45 min) three times. Next, 1 M NaOH is added to the sediment to increase the pH value to 9. Vigorous agitation and tip sonication are employed to redisperse the particles (no additional water is added besides the 1 mol/L NaOH). This procedure results in a homogeneous dispersion of 35−45 wt % silica particles.

Ternary Mixture Preparation. Ternary mixtures made of DEP (10 vol %), water (40 vol %), and IPA (50 vol %) are prepared using one of the three particle suspensions: pH3-BSNP, pH9-BSNP, and pH9-MaSNP. Different concentrations of di-C_{10}TAB are added to the ternary mixtures. The ternary mixtures are extruded into toluene using a coaxial microfluidic device connected to syringe pumps.[12,22]

Characterization. *Zeta Potential, Surface Charge Density, Dynamic Light Scattering (DLS), and Turbidity Measurements.* Silica nanoparticles are dispersed in water and adjusted to different pH values by adding either NaOH or HCl and left overnight at room temperature to equilibrate. Zeta potentials of particles are measured using a Malvern Zetasizer 2000 instrument at 25 °C, and in cases where surfactants are added, zeta potentials measured as a function of the surfactant concentration. To measure the surface charge density of different silica particles, acid base titrations are conducted using 1 M NaOH or 1 M HCl to titrate the silanized silica (MaSNPs) or bare silica (BSNPs), respectively (see Supporting Information (SI) Note 1). For the particle suspensions with different liquid mixtures (oil, isopropanol, and water), physical properties such as the dielectric constant, density, and viscosity are derived from the literature[25] and used as inputs for the Zetasizer software. DLS measurements are also determined accordingly for the particle suspensions. Turbidity measurements are conducted by using a turbidity meter (2100Qis Portable Turbidity Meter, Hach) to evaluate the degree of transparency or cloudiness of the ternary mixtures.

Surfactant Adsorption Measurements. The pendant drop method was used to determine air−water surface tensions, by using an optical tensiometer. All vessels were thoroughly cleaned by etching with KOH saturated IPA (base bath) and then rinsing with DI water. Different concentrations of di-C_{10}TAB were mixed with aqueous suspensions, with or without particles. With particles, the supernatant was collected

https://dx.doi.org/10.1021/acs.jpcc.0c01440
J. Phys. Chem. C 2020, 124, 12417−12423

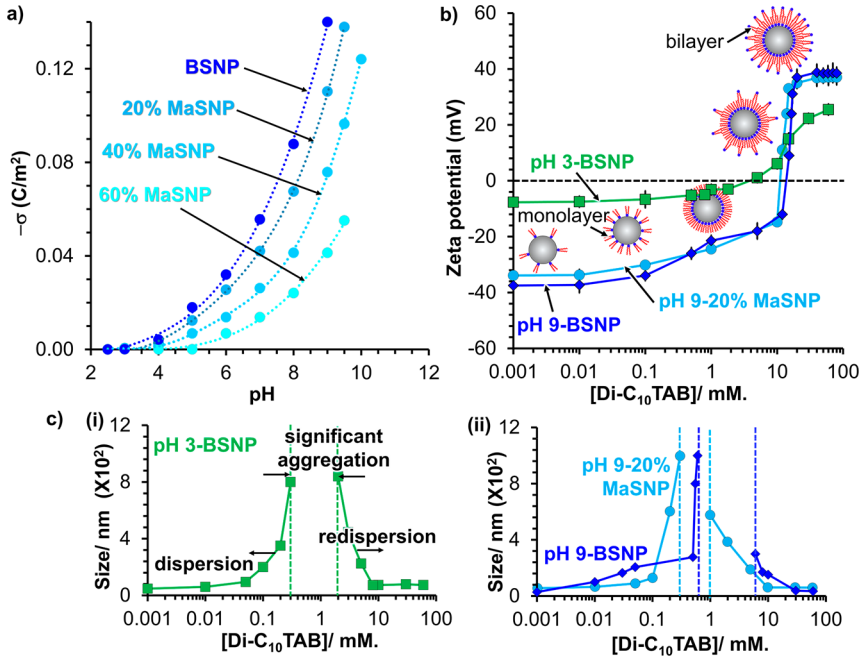

Figure 2. Surface charge densities and colloidal stability of *in situ* modified silica particles in water. (a) Effect of particle pH and silane density on silica surface charge density (see SI Note 1). (b) Zeta potential measurements of silica particles interacting with di-C_{10}TAB in aqueous suspensions. (c) DLS results showing the average sizes of the silica particles interacting with di-C_{10}TAB (SI Note S2).

after strong centrifugation (at 8000 rcf, 20 min) and used for surface tensions. In cases where the effect of alcohol is studied, different volume fractions of isopropanol are mixed with water (with or without particles), and surface tensions are measured after particle removal. Each measurement is conducted three times, with a deviation within ±0.1 mN m^{-1}.

Microscopy. Bijel structures are visualized using confocal laser scanning microscopy (CLSM). The extruded fibers are transferred to a solution of Nile red in hexane. The fluorescence signal from hexane in micrographs displayed in the manuscript have been inverted to visualize the water channels.

RESULTS AND DISCUSSION

Part 1: *In Situ* Modification in Water. Our work of determining the criteria to generate bijels with silica particles of different charge densities begins by investigating the particle properties in water as the dispersion medium. The stabilization of bijels requires particles with partially hydrophobic surfaces. However, silica particles are hydrophilic due to the polar nature of the surface silanol groups. Nevertheless, the silanol groups can serve as adsorption sites for cationic surfactants. The surfactant adsorption results in two effects, (i) the modification of the particle wettability and (ii) the change of the colloidal stability.

We investigate both effects for the adsorption of the cationic double chain surfactant, di-C_{10}TAB, on silica particles (Figure 1a-i). Here, di-C_{10}TAB is paired with three different types of silica nanoparticles (SNPs): (i) Ludox TMA particles at pH 3 (pH3-bare (B)SNP), (ii) Ludox TM-50 particles at pH 9 (pH9-BSNP), and (iii) Ludox TM-50 nanoparticles with 20% of the silanol groups functionalized with TPMA at pH 9 (pH9-methacrylated (Ma)SNP) as illustrated in Figure 1a-ii. TPMA functionalization was characterized in detail within our previous work.[22]

The modification of the particle wettability is reflected in the emulsification behavior. Hydrophilic particles typically form oil-in-water (O/W), and hydrophobic particles typically form water-in-oil (W/O) emulsions. For di-C_{10}TAB concentrations below 1.8 mM, all three particle types stabilize O/W emulsions. Interestingly, phase inversions to W/O occurs at higher di-C_{10}TAB concentrations (18 mM) for all particle types. However, only BSNP-pH9 and MaSNP-pH9 undergo a second (double) phase inversion forming a W/O/W emulsion at even higher di-C_{10}TAB concentrations (Figure 1b). To understand the emulsion behavior, surface charge density, zeta potential, and dynamic light scattering measurements are performed next.

First, we analyze the reduction in surface charge density (σ) on the particles by methacrylate functionalization in the absence of surfactants via acid base titrations (see SI Note 1). Figure 2a shows that increasing the pH of silica particles increases their negative surface charge due to the deprotonation of surface silanol (SiOH) groups. Nonmodified, bare silica nanoparticles at pH 9 (pH9-BSNP) have surface charge densities of ∼−0.14 C/m^2, in good agreement with the literature.[26] pH9-MaSNP have a surface charge density of −0.11 C/m^2. With an increasing degree of methacrylate functionalization, the surface charge density decreases proportionally. Since the reduction of the surface charge density only accounts to ∼20% in comparison to the unmodified particles, we consider pH9-20%methacrylated (Ma)SNP as strongly charged particles.

Zeta potential measurements show the dependency of di-C_{10}TAB modification on the surface charge density of the particles (Figure 2b). At low di-C_{10}TAB concentrations, the absolute value of the zeta potential of pH3-BSNP is significantly lower than for pH 9 particles, demonstrating the higher particle surface charge of pH9-BSNP and pH9-20% MaSNP. For all particles, the zeta potential undergoes inversion from negative to positive (isoelectric point, IEP)

https://dx.doi.org/10.1021/acs.jpcc.0c01440
J. Phys. Chem. C 2020, 124, 12417−12423

upon increasing the di-C_{10}TAB concentration. Above the IEP, di-C_{10}TAB forms a double layer on the particles due to the hydrophobic effect.[27] The zeta potential becomes positive, because the cationic quaternary ammonium groups of the adsorbed surfactants exceed the negative surface charge of the silica. This happens at ∼10 mM di-C_{10}TAB for both pH9-BSNP and pH9-MaSNP and at ∼2 mM di-C_{10}TAB for pH 3-BSNP due to the lower charge density. Dynamic light scattering (DLS) shows that all three particle types aggregate when the di-C_{10}TAB concentration approaches the IEP, indicating the reduced electrostatic repulsion. However, above the IEP, the particles disperse again due to the strong positive surface charge imparted by the surfactant double layer (Figure 2c).

It is possible that another mechanism called "depletion attraction" contributes to the aggregation of particles based on the formation of free surfactant micelles after bilayer formation. However, due to the adsorption of cationic surfactants on the negatively charged silica particles, the availability of free surfactant micelles causing depletion is limited to higher surfactant concentrations following saturated bilayer formation.[28]

The adsorption of cationic surfactant molecules on the surface of negatively charged silica increases their surface charge density. This is based on the principle of screening, which causes further dissociation of the silanol (SiOH) groups to create more SiO^-.[29]

The stronger adsorption of di-C_{10}TAB on the pH 9 particles compared to pH3-BSNP can be quantified via surface tension measurements. To this end, aqueous suspensions at a constant particle concentration and different di-C_{10}TAB concentrations are prepared. The particles are separated by centrifugation, and the air−water surface tension of the supernatant is measured via the pendant drop method. For di-C_{10}TAB alone, the interfacial tension decreases until the critical micelle concentration (cmc) at ∼1.8 mM (Figure 3a, black circles). However, for the supernatants after particle separation, a shift of the surface tension is observed (Figure 3a, green squares and blue diamonds).

The shift of the surface tension results from depletion of di-C_{10}TAB from the solution due to adsorption on the particles. At a given di-C_{10}TAB concentration, the supernatant of the pH9-BSNP has a higher surface tension than the supernatant of the pH3-BSNP. This can be explained by the larger adsorption of di-C_{10}TAB on pH9-BSNP. The adsorption isotherms are derived from this data and plotted in Figure 3b (see SI Note S3). We express the adsorption in molecules per nm^2, allowing for a straightforward comparison with the typical silanol group density on silica of 4 silanol groups per nm^2. For both, particles at pH 9 and at pH 3, the amount of adsorbed di-C_{10}TAB molecules in the plotted range is always significantly smaller than 4, indicating incomplete monolayer formation. However, whereas the pH9-BSNP show steep adsorption profiles, depicting strong interactions between the surfactants and the particles, the pH 3 particles show significantly less surfactant adsorption, reflecting their low surface charge density.

We have seen how the di-C_{10}TAB adsorption can be moderated via the pH value. Next, we demonstrate that the particle TPMA surface functionalization can also moderate the di-C_{10}TAB adsorption at a constant pH value of 9. Figure 3c shows the dependency of the surface tension for supernatants of pH9-MaSNP with different degrees of TPMA functionalization (expressed here as the remaining percentage of silanol groups on the particles). With decreasing TPMA functionalization (40% SiOH, 80% SiOH, 100% SiOH), the surface tension is higher for a given di-C_{10}TAB concentration (Figure 3c). The corresponding adsorption isotherm in Figure 3d shows that increasing the degree of TPMA functionalization reduces the adsorbed amount of di-C_{10}TAB at pH 9 (see SI Note S3).

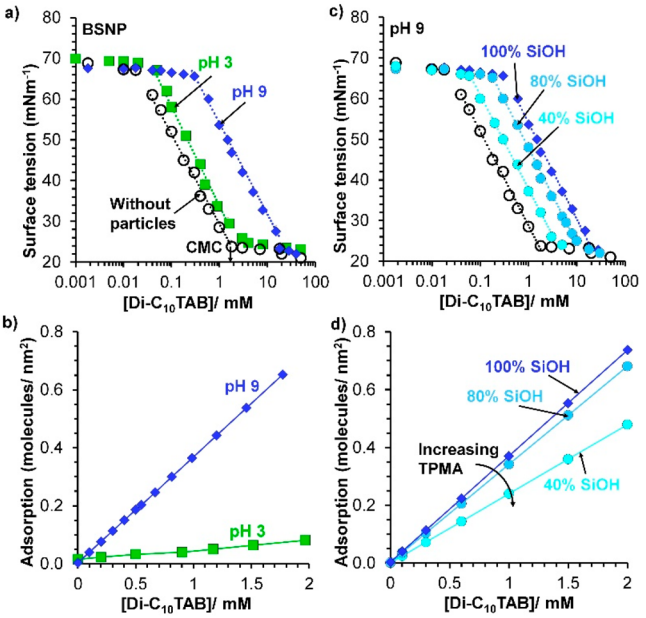

Figure 3. Determination of di-C_{10}TAB adsorption isotherms on the particles. (a) Air−water surface tensions at different di-C_{10}TAB concentrations of water alone (black) and of the supernatant of particle dispersions (green and blue). (b) Surfactant adsorption isotherms for pH3-BSNP and pH9-BSNP. (c) Surface tensions of the supernatants of pH9-MaSNP dispersions with different degrees of residual silanol groups on the particles. (d) Adsorption isotherms derived from surface tensions in (c). The method used to determine the adsorption isotherms is discussed in SI Note S3.

Part 2: *In Situ* Modification in Ternary Liquid Mixtures. Bijel formation via solvent transfer induced phase separation (STrIPS) requires dispersing the particles in a bijel casting mixture.[12] With well dispersed particles, bijels can be stabilized effectively, since the number of particles available for interfacial attachment and jamming is at a maximum.

Figure 4a depicts the ternary phase diagram of water, isopropanol (IPA), and diethyl phthalate (DEP). The ternary composition "A" is the bijel casting mixture, with volumetric fractions of 10% DEP, 40% water, and 50% IPA. For each sample, one of the three different types of silica nanoparticles (pH3-BSNP, pH9-BSNP, and pH9−20%MaSNP) is added through the water fraction, and di-C_{10}TAB is added through the IPA fraction.

Turbidity measurements show that only pH3-BSNP and pH9−20%MaSNP can be dispersed in mixture "A". Turbidity values below 200 nephelometric turbidity units (NTU) in Figure 4b indicate homogeneous particle dispersion as confirmed by complementary dynamic light scattering

https://dx.doi.org/10.1021/acs.jpcc.0c01440
J. Phys. Chem. C 2020, 124, 12417−12423

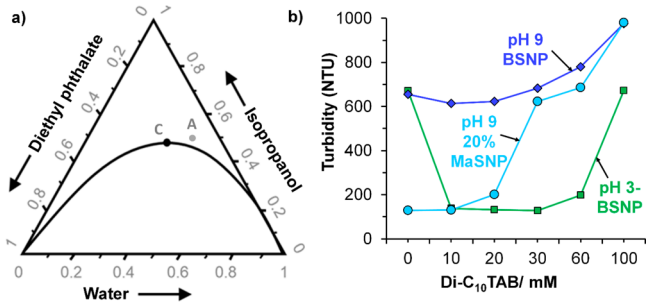

Figure 4. Particle dispersibility in the ternary mixture. (a) Ternary phase diagram depicting mixture "A". (b) Turbidity measurements of ternary mixtures with particles (see SI Note S4).

measurements (SI Note S4). pH3-BSNP disperse in a di-C_{10}TAB concentration range from 10 to 60 mM, while pH9-BSNP do not disperse at any di-C_{10}TAB concentration. In contrast, pH9−20%MaSNP dispersed homogeneously from 0−20 mM di-C_{10}TAB. However, for a higher % of TPMA functionalization, particles aggregate at all di-C_{10}TAB concentrations (see SI Note S4).

What is the difference between pH9-BSNP and the pH9−20%MaSNP, facilitating dispersibility of the latter in mixture "A"? Why do the pH9-BSNP not disperse in mixture "A"? To understand the reason behind particle dispersibility, we analyze the effect of IPA addition on surfactant−particle interactions. We find that the zeta potential curves change drastically in the presence of IPA.[30,31] Figure 5 shows the zeta potentials at variable di-C_{10}TAB concentrations for different IPA volume fractions and silica nanoparticle types.

Three effects of the IPA on the zeta potential are observed: (i) The absolute value of the zeta potential decreases with increasing IPA fraction,[32] (ii) the isoelectric point (IEP) is shifted to higher di-C_{10}TAB concentrations, and (iii) the IEP disappears above 50 vol % IPA. Point (i) can be rationalized based on the reduction of the dielectric constant ε_r of the water upon IPA addition. Lower values of ε_r result in lower degrees of dissociation of the silanol groups, reducing the zeta potentials of the silica particles (see SI Note S5). Point (ii) shows that the onset of di-C_{10}TAB double layer formation takes place at higher concentrations. This can be related to the reduced tendency of the hydrocarbon chains to associate with each other at elevated IPA fractions. The association is driven by the hydrophobic effect, which is diminished in alcohol water mixtures.[30,31] The last point (iii) shows that at 50% IPA, di-C_{10}TAB double layer formation is completely inhibited, which can be explained analogously to point (ii).[33,34]

IPA affects the zeta potential curves similarly for all three particle types. Comparing pH3-BSNP and pH9-BSNP shows that the main difference is the magnitude of the effect. On the other hand, comparing pH9-BSNP with pH9−20%MaSNP shows only small differences, such as the additional decrease of the absolute zeta potential for pH9-BSNP between 10−100 mM. To understand the significantly different colloidal behavior of the particles in the ternary mixture, we analyze the adsorption isotherms of di-C_{10}TAB via surface tension measurements (Figure 6 and SI Note S6).

Our analysis shows the difference of the di-C_{10}TAB adsorption on pH9−20%MaSNP vs pH9-BSNP. For pH9-BSNP, increasing the IPA volume fraction up to 30 vol % shows no significant effect on the di-C_{10}TAB adsorption (Figure 6a-i). In contrast, for pH9−20%MaSNP, the same increase in the IPA volume fraction decreases the di-C_{10}TAB adsorption significantly (Figure 6a-ii). Although the effect is much weaker for pH3-BSNP, also here an increasing IPA volume fraction reduces the di-C_{10}TAB adsorption (Figure 6a-iii).

We have seen in Figure 4b that high di-C_{10}TAB concentrations cause agglomeration of all particle types investigated here. High di-C_{10}TAB concentrations result in strong surfactant adsorption on the particles. However, for pH9−20%MaSNP, particle dispersibility is possible below 20 mM, and for pH3-BSNP, it is possible below 60 mM di-C_{10}TAB. The adsorption isotherms in Figure 6a-ii,iii shows that the di-C_{10}TAB adsorptions are reduced in these concentration ranges due to the elevated IPA volume fraction. For pH3-BSNP, the adsorption is additionally reduced due to the low surface charge density (Figure 6a-iii), and for the strongly charged pH9−20%MaSNP, the adsorption is reduced due to the partial methacrylate functionalization (Figure 6a-ii). In contrast, excessive adsorption of di-C_{10}TAB on the pH9-BSNP results in strong particle aggregation at all di-C_{10}TAB concentrations. This indicates that the dispersibility for pH9−20%MaSNP and pH3-BSNP is related to moderation of the surfactant adsorption by a combined effect of the IPA volume fraction and the reduced adsorption site density on the particle surface.

Last, we investigate the formation of bijels via STrIPS with the three different particle types. Ternary mixtures with the composition "A", including one particle type and variable di-C_{10}TAB concentrations, are extruded into toluene via a coaxial

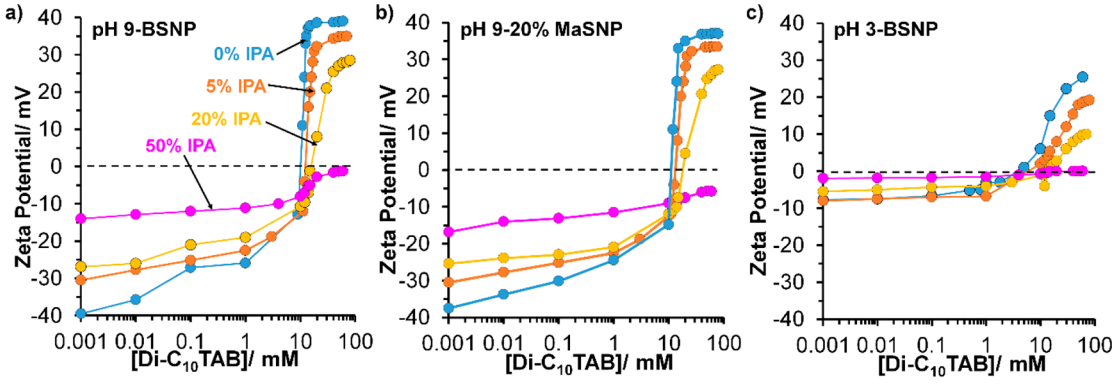

Figure 5. Effect of isopropanol (IPA) volume fraction on zeta potentials measured on different types of silica interacting with di-C_{10}TAB at different concentrations.

https://dx.doi.org/10.1021/acs.jpcc.0c01440
J. Phys. Chem. C 2020, 124, 12417−12423

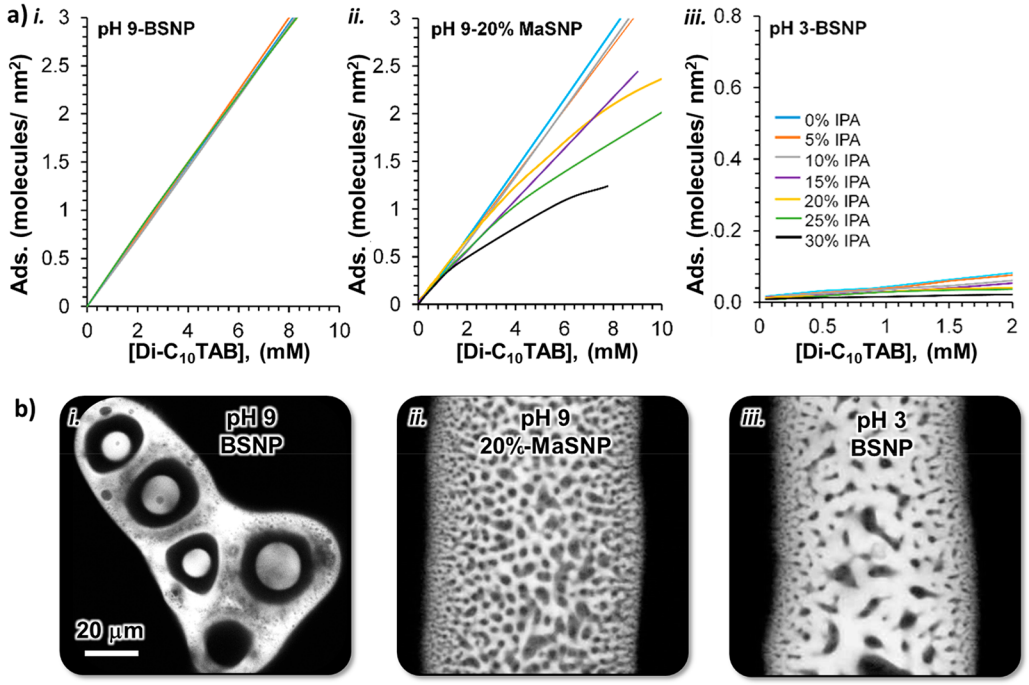

Figure 6. Moderation of surfactant adsorption for bijel stabilization. (a) Surfactant adsorption isotherms on different types of silica depending on the volume fraction of isopropanol. (b) Confocal microscopy of emulsions generated by STrIPS with the three different particle types.

microfluidic glass capillary device.[12] For pH3-BSNP and pH9−20%MaSNP, this results in the formation of continuous fibers. In contrast, for pH9-BSNP, discrete emulsion droplets are formed. Confocal microscopy is used to analyze the morphology of the samples and is shown in Figure 6b.

Both pH3-BSNP and pH9−20%MaSNP allow for the generation of bijels (Figure 6b-ii,iii). Interestingly, for pH9−20%MaSNP, a significantly lower di-C_{10}TAB concentration (~15 mM) is needed for bijel stabilization as compared to pH3-BSNP (~45 mM). This likely results from the higher adsorption density of di-C_{10}TAB on the highly charged silica particles. In contrast, the pH9-BSNP system does not allow for bijel formation at any di-C_{10}TAB concentration, likely because of the strong silica particle agglomeration in the ternary mixture. Instead, multiple emulsion droplets are formed (Figure 6b-i).[35]

CONCLUSIONS

In summary, this paper demonstrates the formation of STrIPS bijels with strongly charged silica nanoparticles. Generating bijels with charged particles is important for applications in catalysis and electrokinetic fluid transport. We describe a method to disperse charged silica nanoparticles in the bijel casting mixture composed of isopropanol (IPA), diethyl phthalate (DEP), and water. We find that a partial surface functionalization of the silica particles with 3-trimethoxypropyl methacrylate (TPMA) facilitates homogeneous dispersibility in the casting mixture. *In situ* surface modification of the particles with didecyldimethylammonium bromide (di-C_{10}TAB) renders them sufficiently hydrophobic to stabilize the bijel. Our measurements show that moderating the adsorption of di-C_{10}TAB on the particles is crucial to enable particle dispersibility and bijel formation. This realization may facilitate the formation of bijels with other strongly charged particle materials besides silica via moderated *in situ* particle modification, broadening the application potentials of bijels. Our current research explores electrokinetic fluid transport in bijels made with highly charged silica particles for applications in biphasic reactions and separations.

ASSOCIATED CONTENT

Supporting Information

The Supporting Information is available free of charge at https://pubs.acs.org/doi/10.1021/acs.jpcc.0c01440.

Colloidal stability of silica particles interacting with surfactants in water, determination of surface charge on silica particles, method for calculating surfactant adsorption isotherms, particle dispersibility in ternary mixtures, effect of isopropanol on silica zeta potential measurements, surface tension measurements used to derive the nature of adsorptions of surfactants on different types of silica (PDF)

AUTHOR INFORMATION

Corresponding Author

Martin F. Haase − *Department of Chemical Engineering, Rowan University, Glassboro, New Jersey 08028, United States; Van't Hoff Laboratory for Physical and Colloidal Chemistry, Debye Institute for Nanomaterial Science, Utrecht University, Utrecht 3584 CH, The Netherlands;* orcid.org/0000-0002-1355-151X; Phone: +31(0)3-02532547; Email: m.f.haase@uu.nl

Authors

Stephen Boakye-Ansah − *Department of Chemical Engineering, Rowan University, Glassboro, New Jersey 08028, United States*

Mohd Azeem Khan − *Van't Hoff Laboratory for Physical and Colloidal Chemistry, Debye Institute for Nanomaterial Science, Utrecht University, Utrecht 3584 CH, The Netherlands*

Complete contact information is available at: https://pubs.acs.org/10.1021/acs.jpcc.0c01440

https://dx.doi.org/10.1021/acs.jpcc.0c01440
J. Phys. Chem. C 2020, 124, 12417−12423

Notes

The authors declare no competing financial interest.

■ ACKNOWLEDGMENTS

This project has received funding from the European Research Council (ERC) under the European Union's Horizon 2020 research and innovation programme (Grant agreement No. 802636). S.B.-A. is supported by NSF career award 1751479.

■ REFERENCES

(1) Witt, J. A.; Mumm, D. R.; Mohraz, A. Microstructural Tunability of Co-Continuous Bijel-Derived Electrodes to Provide High Energy and Power Densities. *J. Mater. Chem. A* **2016**, *4* (3), 1000−1007.
(2) Cai, D.; Richter, F. H.; Thijssen, J. H. J.; Bruce, P. G.; Clegg, P. S. Direct Transformation of Bijels into Bicontinuous Composite Electrolytes Using a Pre-Mix Containing Lithium Salt. *Mater. Horiz.* **2018**, *5* (3), 499−505.
(3) Zekoll, S.; Marriner-Edwards, C.; Hekselman, A. K. O.; Kasemchainan, J.; Kuss, C.; Armstrong, D. E. J.; Cai, D.; Wallace, R. J.; Richter, F. H.; Thijssen, J. H. J.; Bruce, P. G. Hybrid Electrolytes with 3D Bicontinuous Ordered Ceramic and Polymer Microchannels for All-Solid-State Batteries. *Energy Environ. Sci.* **2018**, *11* (1), 185−201.
(4) Haase, M. F.; Jeon, H.; Hough, N.; Kim, J. H.; Stebe, K. J.; Lee, D. Multifunctional Nanocomposite Hollow Fiber Membranes by Solvent Transfer Induced Phase Separation. *Nat. Commun.* **2017**, *8* (1), 1234.
(5) Thorson, T. J.; Gurlin, R. E.; Botvinick, E. L.; Mohraz, A. Bijel-Templated Implantable Biomaterials for Enhancing Tissue Integration and Vascularization. *Acta Biomater.* **2019**, *94*, 173−182.
(6) Imperiali, L.; Clasen, C.; Fransaer, J.; Macosko, C. W.; Vermant, J. A Simple Route towards Graphene Oxide Frameworks. *Mater. Horiz.* **2014**, *1* (1), 139−145.
(7) Santiago Cordoba, M. A.; Spendelow, J. S.; Parra-Vasquez, A. N. G.; Kuettner, L. A.; Welch, P. M.; Hamilton, C. E.; Oertel, J. A.; Duque, J. G.; Meierdierks, E. J.; Semelsberger, T. A.; Gordon, J. C.; Lee, M. N. Aerobijels: Ultralight Carbon Monoliths from Cocontinuous Emulsions. *Adv. Funct. Mater.* **2020**, *30* (6), 2070040.
(8) Di Vitantonio, G.; Wang, T.; Haase, M. F.; Stebe, K. J.; Lee, D. Robust Bijels for Reactive Separation via Silica-Reinforced Nanoparticle Layers. *ACS Nano* **2019**, *13* (1), 26−31.
(9) Cha, S.; Lim, H. G.; Haase, M. F.; Stebe, K. J.; Jung, G. Y.; Lee, D. Bicontinuous Interfacially Jammed Emulsion Gels (Bijels) as Media for Enabling Enzymatic Reactive Separation of a Highly Water Insoluble Substrate. *Sci. Rep.* **2019**, *9* (1), 6363.
(10) Herzig, E. M.; White, K. A.; Schofield, A. B.; Poon, W. C. K.; Clegg, P. S. Bicontinuous Emulsions Stabilized Solely by Colloidal Particles. *Nat. Mater.* **2007**, *6* (12), 966−971.
(11) Jansen, F.; Harting, J. From Bijels to Pickering Emulsions: A Lattice Boltzmann Study. *Phys. Rev. E - Stat. Nonlinear, Soft Matter Phys.* **2011**, *83* (4), 046707.
(12) Haase, M. F.; Stebe, K. J.; Lee, D. Microparticles: Continuous Fabrication of Hierarchical and Asymmetric Bijel Microparticles, Fibers, and Membranes by Solvent Transfer-Induced Phase Separation (STRIPS) (Adv. Mater. 44/2015). *Adv. Mater.* **2015**, *27* (44), 7065−7071.
(13) Lee, M. N.; Mohraz, A. Bicontinuous Macroporous Materials from Bijel Templates. *Adv. Mater.* **2010**, *22* (43), 4836−4841.
(14) Cai, D.; Clegg, P. S.; Li, T.; Rumble, K. A.; Tavacoli, J. W. Bijels Formed by Direct Mixing. *Soft Matter* **2017**, *13* (28), 4824−4829.
(15) Huang, C.; Forth, J.; Wang, W.; Hong, K.; Smith, G. S.; Helms, B. A.; Russell, T. P. Bicontinuous Structured Liquids with Sub-Micrometre Domains Using Nanoparticle Surfactants. *Nat. Nanotechnol.* **2017**, *12*, 1060−1063.
(16) Koretsky, A. F.; Kruglyakov, P. M. *Izv. Sib. Otd. Akad. Nauk USSR* **1971**, *2*, 139.
(17) Aveyard, R.; Binks, B. P.; Clint, J. H. Emulsions Stabilised Solely by Colloidal Particles. *Adv. Colloid Interface Sci.* **2003**, *100−102*, 503−546.
(18) Stratford, K.; Adhikari, R.; Pagonabarraga, I.; Desplat, J. C.; Cates, M. E. Chemistry: Colloidal Jamming at Interfaces: A Route to Fluid-Bicontinuous Gels. *Science (Washington, DC, U. S.)* **2005**, *309* (5744), 2198−2201.
(19) Tavacoli, J. W.; Thijssen, J. H. J.; Schofield, A. B.; Clegg, P. S. Novel, Robust, and Versatile Bijels of Nitromethane, Ethanediol, and Colloidal Silica: Capsules, Sub-Ten-Micrometer Domains, and Mechanical Properties. *Adv. Funct. Mater.* **2011**, *21* (11), 2020−2027.
(20) Bai, L.; Fruehwirth, J. W.; Cheng, X.; Macosko, C. W. Dynamics and Rheology of Nonpolar Bijels. *Soft Matter* **2015**, *11* (26), 5282−5293.
(21) Tran, L.; Haase, M. F. Templating Interfacial Nanoparticle Assemblies via in Situ Techniques. *Langmuir* **2019**, *35* (26), 8584−8602.
(22) Boakye-Ansah, S.; Schwenger, M. S.; Haase, M. F. Designing Bijels Formed by Solvent Transfer Induced Phase Separation with Functional Nanoparticles. *Soft Matter* **2019**, *15* (16), 3379−3388.
(23) Haase, M. F.; Sharifi-Mood, N.; Lee, D.; Stebe, K. J. In Situ Mechanical Testing of Nanostructured Bijel Fibers. *ACS Nano* **2016**, *10* (6), 6338−6344.
(24) Zeng, S.; Chen, C. H.; Mikkelsen, J. C.; Santiago, J. G. Fabrication and Characterization of Electroosmotic Micropumps. *Sens. Actuators, B* **2001**, *79* (2−3), 107−114.
(25) Yang, R.; Wang, F.; Blunk, R. H.; Angelopoulos, A. P. Competing Effects of Silanol Surface Concentration and Solvent Dielectric Constant on Electrostatic Layer-by-Layer Assembly of Silica Nanoparticles on Gold. *J. Colloid Interface Sci.* **2010**, *349* (1), 148−152.
(26) Lagström, T.; Gmür, T. A.; Quaroni, L.; Goel, A.; Brown, M. A. Surface Vibrational Structure of Colloidal Silica and Its Direct Correlation with Surface Charge Density. *Langmuir* **2015**, *31* (12), 3621−3626.
(27) Chandler, D. Interfaces and the Driving Force of Hydrophobic Assembly. *Nature* **2005**, *437* (7059), 640−647.
(28) Furusawa, K.; Sato, A.; Shirai, J.; Nashima, T. Depletion Flocculation of Latex Dispersion in Ionic Micellar Systems. *J. Colloid Interface Sci.* **2002**, *253* (2), 273−278.
(29) Goloub, T. P.; Koopal, L. K.; Bijsterbosch, B. H.; Sidorova, M. P. Adsorption of Cationic Surfactants on Silica. Surface Charge Effects. *Langmuir* **1996**, *12* (13), 3188−3194.
(30) Esumi, K.; Ikemoto, M.; Meguro, K. Effect of Surfactant on the Dispersion of Alumina in Water-Alcohol Mixtures. *Colloids Surf.* **1990**, *46* (2), 231−237.
(31) Esumi, K.; Kobayashi, T.; Meguro, K. Characterization of the Surfactant Layer on Alumina in Water-Dioxane Mixtures. *Colloids Surf.* **1991**, *54*, 189−196.
(32) Kosmulski, M.; Matijević, E. ζ-Potentials of Silica in Water-Alcohol Mixtures. *Langmuir* **1992**, *8* (4), 1060−1064.
(33) Reekmans, S.; Luo, H.; Van der Auweraer, M.; De Schryver, F. C. Influence of Alcohols and Alkanes on the Aggregation Behavior of Ionic Surfactants in Water. *Langmuir* **1990**, *6* (3), 628−637.
(34) Shah, S. K.; Chatterjee, S. K.; Bhattarai, A. Micellization of Cationic Surfactants in Alcohol — Water Mixed Solvent Media. *J. Mol. Liq.* **2016**, *222*, 906−914.
(35) Haase, M. F.; Brujic, J. Tailoring of High-Order Multiple Emulsions by the Liquid-Liquid Phase Separation of Ternary Mixtures. *Angew. Chem.* **2014**, *126* (44), 11987−11991.

https://dx.doi.org/10.1021/acs.jpcc.0c01440
J. Phys. Chem. C 2020, 124, 12417−12423